January 2017

The small heat shock proteins αB-crystallin (HSPB5) and Hsp27 (HSPB1) inhibit the intracellular aggregation of α-synuclein

Dezerae Cox
University of Wollongong, dcc356@uowmail.edu.au

Heath Ecroyd
University of Wollongong, heathe@uow.edu.au

The small heat shock proteins αB-crystallin (HSPB5) and Hsp27 (HSPB1) inhibit the intracellular aggregation of α-synuclein

Abstract

Protein homeostasis, or proteostasis, is the process of maintaining the conformational and functional integrity of the proteome. Proteostasis is preserved in the face of stress by a complex network of cellular machinery, including the small heat shock molecular chaperone proteins (sHsps), which act to inhibit the aggregation and deposition of misfolded protein intermediates. Despite this, the pathogenesis of several neurodegenerative diseases has been inextricably linked with the amyloid fibrillar aggregation and deposition of α-synuclein (α-syn). The sHsps are potent inhibitors of α-syn aggregation in vitro. However, the limited availability of a robust, cell-based model of α-syn aggregation has, thus far, restricted evaluation of sHsp efficacy in the cellular context. As such, this work sought to establish a robust model of intracellular α-syn aggregation using Neuro-2a cells. Aggregation of α-syn was found to be sensitive to inhibition of autophagy and the proteasome, resulting in a significant increase in the proportion of cells containing α-syn inclusions. This model was then used to evaluate the capacity of the sHsps, αB-c and Hsp27, to prevent α-syn aggregation in cells. To do so, we used bicistronic expression plasmids to express the sHsps. Unlike traditional fluorescent fusion constructs, these bicistronic expression plasmids enable only individual transfected cells expressing the sHsps (via expression of the fluorescent reporter) to be analysed, but without the need to tag the sHsp, which can affect its oligomeric structure and chaperone activity. Overexpression of both αB-c and Hsp27 significantly reduced the intracellular aggregation of α-syn. Thus, these findings suggest that overexpressing or boosting the activity of sHsps may be a way of preventing amyloid fibrillar aggregation of α-syn in the context of neurodegenerative disease.

Disciplines

Medicine and Health Sciences

Publication Details

Cox, D. & Ecroyd, H. (2017). The small heat shock proteins αB-crystallin (HSPB5) and Hsp27 (HSPB1) inhibit the intracellular aggregation of α-synuclein. Cell Stress and Chaperones, 22 (4), 589-600.

The small heat shock proteins αB-crystallin (HSPB5) and Hsp27 (HSPB1) inhibit the intracellular aggregation of α-synuclein

Dezerae Cox[1,2] and Heath Ecroyd[1,2]

[1] Illawarra Health and Medical Research Institute and [2] School of Biological Sciences, University of Wollongong, Wollongong, New South Wales, 2522, Australia

To whom correspondence should be addressed:

Associate Professor Heath Ecroyd, Illawarra Health and Medical Research Institute, University of Wollongong, Northfields Avenue, Wollongong, NSW 2522,

Telephone: 02 4221 3443

Email: heathe@uow.edu.au

Keywords: molecular chaperones, amyloid fibrils, protein inclusions, bicistronic vectors, proteostasis

Abbreviations: α-syn - α-synuclein; αB-c - αB-crystallin; BSA - bovine serum albumin; FBS - foetal bovine serum; sHsp - small Heat shock protein

Acknowledgements: DC is supported by an Australian Postgraduate Award. HE was supported by an Australian Research Council Future Fellowship (FT110100586). This work was supported by grants from the Australian Department of Health and Ageing and the University of Wollongong. We thank Dr Tracey Berg (University of Wollongong, Australia) for help developing the bicistronic constructs used in this work and the Illawarra Health and Medical Research Institute for technical support.

Abstract

Protein homeostasis, or proteostasis, is the process of maintaining the conformational and functional integrity of the proteome. Proteostasis is preserved in the face of stress by a complex network of cellular machinery, including the small heat shock molecular chaperone proteins (sHsps), which act to inhibit the aggregation and deposition of misfolded protein intermediates. Despite this, the pathogenesis of several neurodegenerative diseases has been inextricably linked with the amyloid fibrillar aggregation and deposition of α-synuclein (α-syn). The sHsps are potent inhibitors of α-syn aggregation *in vitro*. However, the limited availability of a robust, cell-based model of α-syn aggregation has, thus far, restricted evaluation of sHsp efficacy in the cellular context. As such, this work sought to establish a robust model of intracellular α-syn aggregation using Neuro-2a cells. Aggregation of α-syn was found to be sensitive to inhibition of autophagy and the proteasome, resulting in a significant increase in the proportion of cells containing α-syn inclusions. This model was then used to evaluate the capacity of the sHsps, αB-c and Hsp27, to prevent α-syn aggregation in cells. To do so, we used bicistronic expression plasmids to express the sHsps. Unlike traditional fluorescent fusion constructs, these bicistronic expression plasmids enable only individual transfected cells expressing the sHsps (via expression of the fluorescent reporter) to be analysed, but without the need to tag the sHsp, which can affect its oligomeric structure and chaperone activity. Overexpression of both αB-c and Hsp27 significantly reduced the intracellular aggregation of α-syn. Thus, these findings suggest that overexpressing or boosting the activity of sHsps may be a way of preventing amyloid fibrillar aggregation of α-syn in the context of neurodegenerative disease.

Introduction

Parkinson's disease (PD) is the second most prevalent form of age-related neurodegenerative disorder, with its world-wide incidence projected to reach at least 8.7 million individuals over 50 years of age by 2030 (de Lau and Breteler 2006, Dorsey et al. 2007, Massano and Bhatia 2012). The pathogenesis of PD, and other neurodegenerative diseases, has been inextricably linked with the amyloid fibrillar aggregation and deposition of α-synuclein (α-syn). The initiation of aggregation in this context results from dysfunction in the cellular defence mechanisms that would otherwise maintain protein homeostasis, or proteostasis. Proteostasis refers to the preservation of proteins in their correct location, concentration and conformation, enabling them to fulfil their biological function (Balch et al. 2008). As such, proteostasis relies on a number of integrated pathways, including those involved in transcription and translation, protein folding, trafficking and compartmentalisation, and finally degradation (Yerbury et al. 2005). Key components of this proteostasis network are the molecular chaperones, which assist proteins in acquiring and maintaining their native conformation.

The small heat shock proteins (sHsps) are a family of molecular chaperones that are among the first and most up-regulated in response to cellular stress. At present, there are ten recognised mammalian sHsps (HSPB1 – HSPB10); the most well characterised are Hsp27 (HSPB1) and αB-crystallin (αB-c; HSPB5) (Kampinga et al. 2009, Carra et al. 2013). The sHsp chaperones are defined by the presence of a conserved, central α-crystallin domain of approximately 90 residues, flanked by variable N- and C-terminal regions (de Jong et al. 1993). In addition, while the sHsps are characterised by a relatively small monomeric mass (typically 12 – 43 kDa), they are known to form oligomeric species which, in the case of Hsp27 and αB-c, are polydisperse and undergo dynamic subunit exchange (Bova et al. 1997, Bova et al. 2000, Van Montfort et al. 2002, Lelj-Garolla and Mauk 2006, Ahmad et al. 2008, Benesch et al. 2008, Jehle et al. 2010, Jehle et al. 2011). The dynamic

exchange of subunits between oligomers is thought to be crucial for the chaperone action of these sHsps.

Both Hsp27 and αB-c have been shown to be potent inhibitors of α-syn aggregation using *in vitro*, solution-based assays (Bruinsma et al. 2011, Cox et al. 2016). However, it remains to be established whether these sHsps can prevent the aggregation of α-syn in cells (Cox et al. 2014). Cell-based models of α-syn aggregation have provided some evidence that sHsps can inhibit α-syn aggregation and/or the toxicity associated with this process (Klucken et al. 2004, Zourlidou et al. 2004, Outeiro et al. 2006). However, an issue with some of these cell-based models of a-syn aggregation, which has hampered their use in quantitative studies, is that only a small proportion of the cells in culture develop inclusions (typically less than 5% in studies where this is has been quantified) (McLean et al. 2001, Klucken et al. 2004, Zourlidou et al. 2004, Outeiro et al. 2006). This severely limits the types of biochemical analyses that can be undertaken with these models. Therefore, in this work we sought to develop a robust, reliable and quantifiable cell-based model of α-syn aggregation in order to examine whether the sHsps Hsp27 and αB-c can inhibit α-syn aggregation in cells.

In developing a model to study sHsp chaperone function in cells we have also considered the impact of attaching a (bulky) fluorescent tag to sHsps. The formation of dynamic oligomers is a characteristic feature of Hsp27 and αB-c (Bova et al. 2000, Van Montfort et al. 2002). Recent work has demonstrated that the addition of a fluorescent protein tag to the N- or C-terminus of αB-c or Hsp27 significantly impacts the ability of these sHsps to form oligomeric assemblies and chaperone activity, compared to the non-labelled protein (Datskevich et al. 2012a, Datskevich et al. 2012b, Datskevich and Gusev 2014). Unfortunately, the expression of untagged sHsps in cells does not readily allow differences in transfection efficiency and expression levels to be taken into account when comparing between individual cells and samples in an experiment, which can confound analyses. We therefore sought an alternate method to evaluate the chaperone activity of sHsps in cells that did not involve tagging them with a fluorescent protein, but does enable differences in

transfection efficiencies and protein expression to be accounted for in downstream analyses. Bicistronic expression constructs enable the simultaneous expression of a gene of interest (in this case a sHsp) and a fluorescent (reporter) protein (in this case EGFP) from the one mRNA. Moreover, the mRNA contains an internal ribosome entry site (IRES) such that the expression of the sHsp of interest and fluorescent protein is correlated. Thus, the levels of the fluorescent protein can act as a reporter of the expression of the gene of interest. Use of IRES constructs therefore allows transfected cells to be detected, and the relative levels of the gene of interest (in this case the sHsp) to be quantified (based on the expression levels of the fluorescent reporter), without the need to add a fluorescent tag directly to the protein.

In this work, we describe the development of a robust and reliable cell-based model of α-syn aggregation. This model was then employed to evaluate the ability of the sHsps Hsp27 and αB-c to prevent a-syn aggregation into inclusions in cells. As the addition of a fluorescent tag potentially impacts the function of sHsps in cells (Datskevich et al. 2012a, Datskevich et al. 2012b, Datskevich and Gusev 2014), bicistronic IRES vectors were used to express Hsp27 or αB-c. Our findings demonstrate that these sHsps are effective in inhibiting the aggregation and deposition of α-syn into inclusions in cells.

Materials and Methods

Materials

All materials used in this work were purchased from Sigma-Aldrich (St. Louis, MO, USA) or Amresco (Solon, OH, U.S.A.) unless otherwise indicated. The pET24a(+) bacterial expression vector, containing the human SNCA (α-syn) gene, was used for expression of recombinant α-syn in chemically competent BL21 (DE3) *E. coli*. Recombinant α-syn was expressed, purified and quantified as described previously (Cox et al. 2016). Seed fibrils were produced from monomeric α-syn as described previously (Brown et al. 2016), and were used to produce mature fibrils. Briefly, recombinant monomeric α-syn (100 μM) was incubated at 37^{o}C in 50 mM phosphate buffer (pH 7.4) in the presence of 1 μM preformed seed fibrils for 48 h.

The pEGFP-N3 mammalian expression vectors, containing the human *SNCA* (*α-syn*) gene with or without the disease-related mutation (A53T), were a gift from Dr. Dean Poutney (Griffith University, Australia), and were used to induce cellular expression of α-syn variants C-terminally tagged with EGFP. The pCMV6-AC-GFP mammalian expression vector, containing M337V TDP-43 cDNA C-terminally tagged with TurboGFP (tGFP), was a gift from Dr. Daniel Whiten (University of Wollongong, Australia). The bicistronic pIRES2-EGFP vector was a kind gift from Dr Lezanne Ooi (University of Wollongong, Australia). Constructs containing αB-c, Hsp27, or the non-chaperone control protein, an 'invisible' isoform of EGFP, EGFP^{inv} (i.e. a non-fluorescent Y66L mutant form of EGFP (Olshina et al. 2010, Ramdzan et al. 2012)), were generated by amplifying genes encoding the genes (with flanking restriction sites) from existing plasmid constructs for sub-cloning upstream of the IRES site of the pIRES2 plasmids; αB-crystallin (*CRYAB*; GenBank NM_001885) with *Nhe*I/*Sal*I, HSP27 (*HSPB1*; GenBank BT019888.1) with *Bgl*II/*Sal*I, and EGFP^{inv} with flanking *Bgl*II/*Eco*RI sites. Sequences of all constructs were verified prior to use.

Mouse neuroblastoma cells (Neuro-2a; N2a) and human embryonic kidney (HEK293) cells were obtained from the American Type Culture Collection (Manassas, VA, U.S.A.). Both cell lines were

routinely tested for mycoplasma contamination every 6 months, and the identity of the human-derived cell line was verified via short tandem repeat (STR) profiling (Garvan Institute of Medical Research, Sydney, Australia). For immunolabelling of α-syn, mouse monoclonal anti-α-syn antibody (clone Syn211) and a peroxidase conjugated anti-mouse IgG secondary antibody were obtained from Sigma-Aldrich (St. Louis, USA). For immunolabelling of sHsps, rabbit polyclonal anti-αBc (ab13497) and anti-Hsp27 (ab5579) antibodies were acquired from Abcam (Cambridge, UK). Goat anti-mouse and anti-rabbit secondary antibodies conjugated to DyLight650 (ab96874 and ab96902 respectively), mouse (ab37355) and rabbit (ab171870) IgG controls were also purchased from Abcam (Cambridge, UK).

Cloning of α-synA53T expression construct*

The cloning strategy was designed according to findings published by McLean and colleagues (2001) (McLean et al. 2001), in which an aggregation-prone cleavage product of α-syn was identified within cells initially transfected to express α-syn with a C-terminal EGFP tag (i.e. α-syn-EGFP). Specifically, this product was approximately 27 kDa, and corresponded to a cleaved form of α-syn-EGFP in which the last 155 residues from the C-terminal region of EGFP were removed. This resulted in α-syn fused to a non-fluorescent fragment of EGFP. The region corresponding to α-synA53T and the first 85 residues of EGFP (i.e. lacking the last 155 residues, designated α-synA53T*) was amplified from the original α-synA53T-EGFP construct by PCR using MyTaq DNA polymerase, the CMV-F primer (5' – CGCAAATGGGCGGTAGGCGTG – 3') and a custom designed primer (5' – CTT**GCGGCCGC**CTAGAAGAAGTCGTGCTGC – 3') containing the NotI restriction site (bold text). PCR was performed using a Mastercycler ProS (Eppendorf) and consisted of 35 cycles, with each cycle consisting of denaturation at 95°C for 15 s, annealing at 55°C for 15 s, and extension at 72°C for 10 s. The amplified product was gel purified, digested using the restriction enzymes Acc65I and NotI, and ligated back into the pEGFP-N3 vector. A clone positive for the α-synA53T* insert was selected and plasmid DNA extracted and sequenced.

Culture and transfection of mammalian cell lines

Mammalian cell lines (N2a and HEK293) were chosen due to the ease with which they can be cultured, transfected and imaged. In addition, N2a cells represent a well-established neuronal model used for characterising aggregation (Krishnan et al. 2006, Ojha et al. 2011, Ormsby et al. 2013, Chai et al. 2016). Cells were cultured in Dulbecco's Modified Eagle's Medium/Ham's Nutrient Mixture F-12 (DMEM/F12; ThermoFischer Scientific, Waltham, USA) supplemented with 10% (v/v) foetal bovine serum (FBS; Bovagen Biologicals, East Keilor, Australia) and 2.5 mM L-glutamine (ThermoFischer Scientific, Waltham, USA). All media was sterile filtered and warmed to 37^{o}C for use. All tissue culture was performed within a laminar flow biosafety cabinet, and cells were incubated in a Heracell 150i CO2 incubator (ThermoFischer Scientific, Waltham, USA) under 5% CO2/95% air at 37^{o}C.

Cells were passaged when at 80% confluency or after a period of 72 h, and reseeded into fresh CELLSTAR flasks or culture plates (both from Greiner Bio-one, Frickenhausen, Germany) where required. For plating purposes, cells were seeded at 100 000 cells/mL in 6-well, 12-well or 24-well plates (Greiner Bio-One, Frickenhausen, Germany), or 8-well chamber slides (Ibidi, Martinsried, Germany) and grown overnight. Cells were then transfected using Lipofectamine® LTX (Invitrogen, Waltham, U.S.A.) according to the manufacturer's instructions. Briefly, DNA:liposome complexes were generated by incubation of 1 µg of plasmid DNA in serum free DMEM/F12 with 3 µL of Lipofectamine® LTX and 1 µL PLUS™ reagent per ~3.5 cm^2 of cells to be transfected, at room temperature for 30 min. In the case of dual transfections, DNA:liposome complexes for each plasmid were prepared separately then combined after the 30 min incubation period to allow mixing. In this way, each plasmid is incorporated into separate liposomes, which can then be independently taken up by cells. Dual transfections were completed at a 1:4 (IRES:α-syn) (w/w) ratio of DNA. DNA complexes were then applied to cells in fresh culture medium and incubated for 48 h at 37°C under 5% CO2/95% air.

Where necessary, cells were treated with various inhibitors of proteostasis pathway components to induce cellular stress. Treatments included a proteasome inhibitor (MG132; 10 μM), an autophagy inhibitor (3-methyladenine (3-MA); 10 mM), an inducer of ER stress (thapsigargin; 3 μM), or an inducer of oxidative stress (FeCl2; 10 mM), all of which were solubilised in DMSO as 1000-times stocks and subsequently diluted into serum free DMEM/F12 for addition to cultured cells. The inhibitor concentrations were selected according to previously reported and commonly used concentrations (Ostrerova-Golts et al. 2000, Fioriti et al. 2005, Földi et al. 2013, Gui et al. 2014, Guo et al. 2016). Mock treated cells were exposed to the appropriate concentration of DMSO in serum free DMEM/F12.

Immunolabelling of α-syn and sHsps

Intracellular α-syn was routinely detected via immunocytochemistry. Cells were seeded at 100 000 cells/mL onto sterilised 19 mm glass coverslips (ProSciTech, Thuringowa, Australia) or in 8-well chamber slides (Ibidi, Martinsried, Germany) and transfected as described above. After 48 h, or following treatment for the times indicated, culture medium was removed from the cells and the cells washed twice with PBS. Cells were fixed via incubation with 4% (w/v) paraformaldehyde (PFA, pH 7.4) for 20 min at room temperature and washed twice with PBS. Cells were then permeabilised using 0.5% (v/v) Triton X-100 in PBS for 20 min at room temperature, before being washed twice with 1% (w/v) BSA in PBS. Cells were then blocked using 5% (w/v) BSA in PBS, and washed twice in 1% (w/v) BSA in PBS-Tween 20 (PBS-T; PBS containing 0.05% (v/v) Tween-20). Immunolabelling of α-syn was achieved using the mouse monoclonal anti-α-syn antibody diluted 1:500 with 1% (w/v) BSA in PBS-T. Alternatively, sHsps were detected using rabbit polyclonal anti-αBc or anti-Hsp27 antibodies diluted 1:500 with 1% (w/v) BSA in PBS-T. Cells were incubated at 37^{o}C for 1 h in a humidity chamber, before being washed three times with 1% (w/v) BSA in PBS-T. The appropriate fluorophore-conjugated secondary antibody was diluted 1:500 with 1% (w/v) BSA in PBS-T, and

applied to the cells. Following incubation at 37^{o}C for 1 h in a humidity chamber, cells were then washed four times with 1% (w/v) BSA in PBS-T.

Confocal microscopy and image analysis

Coverslips with cells containing fluorescent and/or immunolabelled proteins were mounted onto 26 × 76 mm glass slides (ThermoFischer Scientific, Waltham, USA) using Citifluor™ Anti-Fadent Mounting Solutions (9:1 (v/v) ratio of Citifluor™ CFPVOH: Citifluor™ AF100 anti-fadent; ProSciTech, Thuringowa, Australia) and allowed to set at room temperature for 1 h prior to imaging. Alternatively, cells in chamber slides were overlayed with PBS containing 10% (v/v) Citifluor™ AF100 anti-fadent (ProSciTech, Thuringowa, Australia) and imaged immediately. Cells were observed using a Leica TCS SP5 confocal microscope (Leica Microsystems, Wetzlar, Germany). Fluorescent conjugates were excited at 488 nm, 561 nm, or 633 nm by argon, DPS 561, and HeNe lasers, respectively. Fluorescent emissions were acquired by sequential scanning using the Leica Application Suite –Advanced Fluorescence (LAS-AF) software v3 (Leica Microsystems, Wetzlar, Germany). Either photomultiplier tube (PMT) or hybrid (HyD) detectors were selected and custom filter windows set according to the intensity and emission spectrum of the fluorophore of interest. Gains and filter windows were set according to the untransfected and isotype (mouse or rabbit IgG) stained controls using the overflow colour map, such that samples were below the saturation point, background or non-specific fluorescence was not visible and bleed through was eliminated.

Images collected via confocal microscopy were processed manually with ImageJ (National Institutes of Health, Bethesda, U.S.A.) using custom written macro scripts (Supplementary Information, Figure S1). These methods were developed to enable non-subjective quantification of the number of cells with aggregates between samples. Briefly, cell boundaries of individual cells were defined using the brightfield image, and the transfected cells determined automatically via thresholding of the fluorescent image. Cells containing inclusions (visually defined as fluorescent puncta) were manually selected according to the fluorescent image. The percentage of transfected cells (or co-transfected

cells in experiments involving the IRES constructs) with and without inclusions for each treatment was calculated by the custom written Python script. This was completed with at least 50 cells per treatment over four biological repeats. All statistical analyses (unless otherwise stated) were performed using GraphPad Prism v 5 (GraphPad Software Inc., San Diego, USA) software.

Filter-trap assay

In order to confirm the presence of insoluble α-syn inclusions in cells, a filter-trap assay was performed. Cells were transfected, treated with inhibitors where appropriate and harvested. Cell pellets were washed twice in PBS, and then resuspended in lysis buffer (PBS containing 0.5% (v/v) Triton-X 100, pH 7.4, supplemented with 0.5% (v/v) Halt™ Protease and Phosphatase Inhibitor Cocktail). The total protein concentration for each sample was then determined using a Pierce BCA assay (ThermoFischer Scientific, Waltham, USA) according to the manufacturer's instructions. Samples were diluted to 1 mg/mL using lysis buffer and kept on ice until use. In addition, samples containing known concentrations of recombinant monomeric or fibrillar α-syn were similarly prepared in PBS or spiked into lysis buffer and kept on ice.

In order to determine the concentration of α-syn in samples produced following transfection with the α-synA53T* construct, a dot blot was first performed. Samples were spotted onto nitrocellulose membrane, and left to dry at room temperature for 1 h. The membrane was then blocked at room temperature for 1 h in Tris-buffered saline (TBS; 50 mM Tris and 150 mM NaCl, pH 7.5) containing 5% (w/v) skim milk powder. Blots were then incubated overnight at 4^{o}C in TBS-Tween-20 (TBST; TBS containing 0.05% (v/v) Tween-20) containing 5% (w/v) skim milk powder and the mouse monoclonal anti-α-syn antibody (diluted 1:5000). Blots were washed four times in TBST for 10 min with constant agitation, then incubated at room temperature for 1 h in TBST containing 5% (w/v) skim milk powder and the peroxidase-conjugated anti-mouse secondary antibody (diluted 1:5000). Blots were washed as above, and then labelled α-syn was detected using SuperSignal West Pico Chemiluminescent Substrate or SuperSignal West Dura Extended Duration Chemiluminescent Substrate according to

the manufacturer's instructions (ThermoFischer Scientific, Waltham, USA). The membrane was exposed to Amersham Hyperfilm ECL chemiluminescence film (GE Healthcare, Uppsala, Sweden), or directly imaged using a Gel Logic 2200 Pro Imaging System (Carestream Health, Rochester, NY, USA) or Amersham Imager 600 (GE Healthcare, Uppsala, Sweden).

The intensity of spots of interest were analysed using the gel quantification function in ImageJ, and a standard curve of concentration of recombinant α-syn versus spot intensity was generated (Supplementary Information, Figure S2). The concentration of α-syn in the transfected cell extracts was then determined via interpolation from the standard curve and was found to be less than 1 μM.

The Bio-Dot microfiltration apparatus (Bio-Rad, Hercules, CA) was prepared according to the manufacturer's instructions. Briefly, 0.22 μm cellulose acetate membrane (Whatman, Maidstone, UK) and three sheets of Bio-DOT SF filter paper (Bio-Rad, Hercules, CA) were equilibrated in PBS containing 1% (w/v) SDS (pH 7.4) for 10 min at room temperature. The Bio-Dot apparatus was then assembled containing the membrane and filter paper and tightened under vacuum. Each slot for use was rehydrated with 200 μL PBS, which was then filtered under vacuum immediately prior to the addition of 200 μg of the prepared cell lysate or appropriate control samples. Any unused slots were sealed with clear sealing film, and samples filtered under gentle vacuum. Once all samples had been filtered, 200 μL of PBS was added to the sample well and filtered under gentle vacuum. The membrane was then removed and blocked in 5% (w/v) skim milk powder in TBS, before being analysed via the immunoblotting technique described above.

Results

Fluorescently-tagged α-syn isoforms do not readily aggregate in cells

Transfection with fluorescently tagged aggregation-prone proteins is a common method for investigating cellular aggregation, including that of α-syn (McLean et al. 2001, Outeiro et al. 2006). As such, N2a cells were transfected with constructs encoding for α-synWT-EGFP, α-synA53T-EGFP, EGFP (negative control) or TDP-43-tGFP (positive control). Given the importance of the proteostasis network in modulating cellular aggregation, targeting pathways of this network is a common method of inducing the aggregation of proteins into inclusions (Outeiro et al. 2006, Bertoncini et al. 2007, Wan and Chung 2012). As such, transfected cells were incubated in the absence or presence of MG132 (10 μM, proteasome inhibitor), thapsigargin (3 μM, inducer of ER stress) or FeCl2 (10 mM, inducer of oxidative stress). Cells were then imaged via confocal microscopy (Figure 1A), and EGFP-positive cells containing diffuse fluorescence (left box, 1) or fluorescent puncta (right box, 2) were enumerated. The percentage of EGFP-positive cells containing inclusions was then compared with the untreated, EGFP-expressing negative control cells (Figure 1B). As expected, there was a significantly higher ($p<0.001$) proportion of cells expressing TDP-43-tGFP with inclusions (41.5 ± 7.20%) compared to those expressing EGFP (2.92 ± 1.14%). However, expression of α-synWT-EGFP (3.19 ± 1.3%) or α-synA53T-EGFP (6.11 ± 2.49%) did not result in a significant proportion of cells containing inclusions (Figure 1). Moreover, treatment of cells expressing the α-syn-EGFP variants with proteostasis inhibitors had no significant effect on the percentage of cells containing inclusions, such that the proportion of cells expressing α-syn with inclusions remained very low (<10%).

To determine whether the lack of aggregation of α-syn into inclusions was due to the cell line being used (i.e. N2a cells), this experiment was repeated using HEK293 cells (Figure 1C). As expected, treatment of HEK293 cells expressing TDP-43-tGFP with MG132 and thapsigargin significantly ($p<0.001$) increased the proportion of cells with inclusions (36.1 ± 8.56%) compared to cells expressing EGFP alone (5.40 ± 2.45%). However, as seen for N2a cells, there was no significant

difference in the percentage of α-syn-EGFP expressing HEK293 cells containing fluorescent inclusions following treatment with MG132, thapsigargin or $FeCl_2$ compared to cells expressing EGFP alone. In all cases the percentage of transfected cells expressing α-syn-EGFP with inclusions remained very low (<7%). As such, it was concluded that EGFP-tagged α-syn variants do not readily aggregate in cells, and therefore an alternate model was pursued.

α-Syn-A53T readily aggregates to form inclusions in cells*

Previous work attempting to develop a cell model of α-syn aggregation, in which a fluorescently tagged form of α-syn was expressed in human H4 neuroglioma cells, led to the discovery of intracellular puncta which were non-fluorescent but immunoreactive to α-syn (McLean et al. 2001). This work identified a cleavage product of the expressed α-syn-EGFP in these inclusions. This product consisted of α-syn with a C-terminal fragment of EGFP in which the last 155 residues of EGFP has been cleaved from the protein. According to the sequences provided for these cleavage products, a construct was designed for the expression of α-syn fused to a fragment of EGFP (designated α-synA53T*). The propensity of the resulting α-synA53T* to form intracellular inclusions was then investigated in N2a cells. Following transfection, cells were immunostained for α-syn and mounted on glass slides for imaging via confocal microscopy (Figure 2A-D). Qualitative analysis of cells positive for α-syn revealed the formation of fluorescent inclusions in some cells, which appeared to be distributed throughout the cytosol (Figure 2B, D) and at the periphery of cells (Figure 2C, D). The presence of these inclusions in transfected cells was quantified, and the percentage of transfected cells containing inclusions found to be 31 ± 5.5% of the population. Following treatment with the proteostasis inhibitors 3-MA (autophagy inhibitor) or MG132 (proteasome inhibitor), there was a significant increase in the percentage of cells containing inclusions compared to the untreated or DMSO-vehicle treated samples ($p<0.05$; Figure 2E).

In order to confirm the immunoreactive inclusions represent aggregated α-syn, lysates from cells transfected to express α-synA53T* (or an EGFP control) were subjected to filter trap analysis. Filter

trap assays have been used extensively in the past to assess inclusion formation in cells (Chang and Kuret 2008, Juenemann et al. 2015, Nasir et al. 2015). Typically, soluble protein moves through the membrane pores, while aggregated protein is retained on the membrane such that proteins in the aggregates can be detected by immunoblotting. We first established the specificity of this assay for aggregated α-syn. When recombinant monomeric α-syn was added into buffer at concentrations that exceed the level of α-synA53T* expressed in cells (see Supplementary Figure 2), it was not trapped by the filter and therefore was not detected by immunoblotting (Figure 2F). Moreover, no signal was detected when recombinant monomeric α-syn was added to the lysate from untransfected cells, thus demonstrating that monomeric α-syn does not aggregate in the cell lysate as a result of the lysis procedure. Importantly, when recombinant fibrillar α-syn was spiked into buffer or the lysate from untransfected cells it was trapped by the filter and detected when present at levels as low as 0.04 μM (Figure 2F). As expected, no α-syn signal was detected in lysates from mock transfected or EGFP transfected cells (Figure 2G). However, α-syn was detected in cells transfected to express α-synA53T*, confirming that these cells contained aggregated forms of α-syn. Moreover, there was a significant increase in the amount of aggregated α-syn detected in lysates from cells following treatment with the proteostasis inhibitors, thus correlating with the increase in the number of cells with inclusions following this treatment (Figure 2E). Given the formation of α-syn immunoreactive fluorescent inclusions corresponded to the accumulation of aggregated α-syn, and that this accumulation was sensitive to treatment with inhibitors of proteostasis, it was concluded that expression of α-synA53T* in N2a cells is a suitable cell-based model of α-syn aggregation.

Bicistronic IRES constructs enable sHsp-expressing cells to be identified via an EGFP reporter

First, in order to validate the use of the IRES constructs, the over-expression of the sHsps and EGFP reporter was confirmed (Figure 3). N2a cells were transiently transfected with constructs expressing EGFP/αB-c or EGFP/Hsp27. Following incubation for 24 h, cells were probed for sHsp expression with polyclonal primary and fluorescently-conjugated secondary antibodies before being imaged via

confocal microscopy. As expected, mock transfected N2a cells were not immunoreactive, indicating N2a cells do not constitutively express αB-c or Hsp27 (Figure 3A, C). Transfection with the IRES constructs successfully induced expression of EGFP (Figure 3B, D). When probed with sHsp-specific antibodies, EGFP-positive cells were also immunoreactive for αB-c or Hsp27 respectively (Figure 3B, D). Furthermore, this analysis confirms the production of two discrete proteins from the construct, as the EGFP fluorescence was found to be diffuse throughout the nucleus and cytoplasm, whilst the sHsps were only localised to the cytoplasm. Overall these data confirm that transfection of N2a cells with IRES constructs results in the overexpression of the sHsp of interest, and sHsp-expressing cells can be identified via the EGFP reporter.

sHsps inhibit the deposition of α-synA53T into inclusions in cells*

Having developed a cellular model of α-syn aggregation, this model was then used to examine the ability of αB-c and Hsp27 to prevent α-syn aggregation in cells. N2a cells were co-transfected with the α-synA53T* and IRES constructs encoding EGFP and either αB-c, Hsp27 or $EGFP^{inv}$, and incubated in the absence or presence of proteostasis inhibitors. Cells were imaged via confocal microscopy, and those containing αB-c or Hsp27 (or the $EGFP^{inv}$ control) were identified through expression of the fluorescent reporter EGFP (Figure 4A, green). Cells expressing α-synA53T* were identified by immunolabelling of the α-synA53T* with DyLight-650 (Figure 4B, red). This allows identification of cells containing only α-syn (red only), those containing only αB-c or Hsp27 (or the $EGFP^{inv}$ control; green only), and cells of interest (i.e. co-transfected cells that contain both the α-syn and chaperone or control protein, yellow) (Figure 4C). The number of cells containing inclusions was then manually quantified using randomly imaged fields of view and the percentage of co-transfected cells containing inclusions was then calculated and normalised to the EGFP control (Figure 4D). Expression of αB-c was found to significantly reduce the number of cells containing inclusions in untreated cells ($p<0.05$) and in those treated with the proteostasis disruptors thapsigargin and MG132 ($p<0.01$) (Figure 4D). Whilst αB-c also reduced the proportion of cells containing inclusions following

354 treatment with 3-MA, this effect was not found to be significant. Co-transfection with Hsp27 was
355 found to significantly reduce inclusion formation in both the untreated and treated cells expressing
356 α-synA53T* by approximately 30% ($p<0.05$).

357

Discussion

The potent anti-aggregation properties of the sHsps, αB-c and Hsp27, have been well established *in vitro* (Bruinsma et al. 2011, Cox et al. 2016). However, in order to capture the complex factors influencing protein aggregation in the cell, it is essential to complement these *in vitro* studies with cellular models of aggregation. Here we have developed a cell-based model of α-syn aggregation in which α-syn readily aggregates to form inclusions in a significant proportion of transfected cells. We then used this cell-based model to assess the ability of αB-c and Hsp27 to prevent α-syn aggregation in cells. Our work shows that expression of αB-c or Hsp27 significantly decreased the proportion of cells containing α-syn inclusions, even when the cells were treated with inhibitors of autophagy or the proteasome. These data provide strong evidence that the sHsps are potent inhibitors of α-syn aggregation in cells.

Fusion of a fluorescent protein to a protein of interest is a well described method for studying intracellular aggregation and a key element in facilitating high throughput analyses (Ramdzan et al. 2012). Thus, the first approach to study the effect of sHsps on intracellular α-syn aggregation investigated in this work was to tag the α-syn variants with a C-terminal EGFP. Whilst some cells expressing α-syn-EGFP were found to contain aggregates, the proportion of these cells was very low (5 – 10% of cells) and did not increase even in the presence of proteostasis inhibitors or inducers of cell stress, both of which have been previously reported to increase α-syn aggregation in cells (Bertoncini et al. 2007). Thus, it is concluded that the addition of this relatively large (approximately 27 kDa) fluorescent protein to the C-terminus of α-syn (14.5 kDa) likely interferes with the physical properties of α-syn, significantly altering the structure, conformation and/or chemical properties of the protein, such that its propensity to aggregate in cells is low (Crivat and Taraska 2012). In addition, previous studies have demonstrated that expression of α-syn alone (i.e. without a tag) does not result in significant levels of aggregation in cells (Paxinou et al. 2001, Matsuzaki et al. 2004). However, a cellular cleavage product of α-syn-EGFP, in which the last 155 residues of EGFP have

been removed, was found to readily aggregate into inclusions in cells (McLean et al. 2001). In this work we also report that this α-synA53T* protein readily forms inclusions in cells, which are detectable via immunolabelling of α-syn and by filter-trap assay. Notably, a significant proportion of cells transfected to express α-synA53T* developed inclusions (~30%) and this could be significantly increased by treatment of the cells with inhibitors of proteostasis pathways (i.e. the proteasome and autophagy). Moreover, it has been previously demonstrated that the aggregation of α-synA53T* into inclusions is mediated by the α-syn portion of the protein, since when the same fragment of EGFP was fused to other proteins (i.e. tubulin and synaptophysin) and expressed in cells, these cells did not develop aggregates (McLean et al. 2001). Thus, it is likely that the additional EGFP fragment at the C-terminus of α-syn acts to destabilise α-syn and that this is key to recapitulating the cellular aggregation of α-syn associated with disease.

Importantly, C-terminal cleavage products of α-syn (α-synΔC) have been identified *in vivo*. For example, human brain extracts containing pathological α-syn Lewy bodies have significant levels of α-synΔC, which preferentially localises to detergent-insoluble fractions following extraction of protein aggregates (Li et al. 2005). Moreover, C-terminal truncation of α-syn significantly increases its aggregation propensity when compared to full length α-syn when assessed using *in vitro* ThT-based aggregation assays (Hoyer et al. 2004, Li et al. 2005). In addition, the incorporation of substoichiometric ratios of α-synΔC variants significantly enhances the aggregation of cellular aggregation of full length α-syn (Li et al. 2005). Finally, α-synΔC variants increase the vulnerability of cells in culture to toxic assault by oxidative stressors (Kanda et al. 2000). Together, these data indicate that the C-terminal region of α-syn plays a critical role in governing its propensity to aggregate. Thus, this may account, at least in part, for the increased propensity of α-synA53T* to form inclusions in cells. A cell model that incorporates co-expression of full-length α-syn with an α-synΔC isoform may also result in a robust cellular model of α-syn aggregation.

Whilst this work demonstrated that αB-c and Hsp27 can prevent a-syn aggregation in cells, the molecular mechanism(s) by which this occurs remains to be established. These sHsps may interact with monomeric aggregation-prone α-syn to prevent the formation of oligomeric nuclei, as has been observed in solution-based experiments [17]. Alternatively, sHsps may bind to small α-syn oligomers and, in doing so, prevent growth of these oligomers into fibrillar species that would otherwise lead to their deposition into inclusions. sHsps may also interact with fibrillar α-syn in order to prevent secondary nucleation processes that would otherwise increase the amount of aggregated material and enhance deposition of α-syn into inclusions. It is most likely that the inhibition of α-syn inclusion formation by αB-c and Hsp27 is due to a combination of these mechanisms. Importantly, even in the presence of proteostasis inhibitors, the sHsps successfully inhibited the formation of α-syn inclusions. This suggests that the sHsp mechanism of action is independent of these protein degraadation pathways, and implies that the sHsps most likely inhibit inclusion formation by preventing the initial aggregation of α-syn, rather than promoting its degradation via the ubiquitin-proteasome system or autophagy. Development of techniques that enable the aggregation state of α-syn to be tracked in cells so that this can be linked to specific biological outcomes would greatly assist future work in this area. For example, the development of conformational sensors of α-syn capable of distinguishing monomeric, oligomeric and fibrillar species, such as those developed for Htt (Ormsby et al. 2013), would facilitate investigation of the precise mechanism(s) by which sHsps act to prevent α-syn aggregation in cells.

An important aspect of this work was the use of biscistronic vectors for the expression of the sHsps (and an 'invisible', non-fluorescent variant of EGFP, $EGFP^{inv}$ as a control). These constructs enabled the chaperone activity of the sHsps to be evaluated without the confounding effects of associated with tagging them with a bulky fluorescent protein. Traditional fluorescent fusion approaches to monitor chaperones in cells have been shown to impact the ability of sHsps to form oligomeric assemblies and undergo subunit exchange, processes which are crucial for chaperone efficacy (Datskevich et al. 2012a, Datskevich et al. 2012b, Datskevich and Gusev 2014). However, the

433 bicistronic expression system provides a method to distinguish cells containing the chaperone of
434 interest without adversely affecting the oligomeric and dynamic nature of these proteins. These
435 bicistronic constructs are therefore advantageous for studying sHsp function in cells. This approach
436 could also be used to study other proteins in cells whose structure and/or function may be adversely
437 affected by the addition of a fluorescent protein tag.

438 In summary, in this work we report on a cell-based model of α-syn aggregation and, using this
439 model, demonstrate that the sHsps, Hsp27 and αB-c, prevent the aggregation of α-syn into
440 inclusions in cells. By exploiting a bicistronic vector, sHsp expression and function was able to be
441 assessed in individual cells without the need for a fluorescent tag, which can otherwise compromise
442 the structure and activity of these oligomeric and dynamic chaperone proteins. This work indicates
443 that the sHsps are valid therapeutic targets for aggregation-based diseases such as the α-
444 synucleinopathies.

445 ***References***

446 Ahmad, MF, Raman, B, Ramakrishna, T and Rao, CM (2008). Effect of phosphorylation on αb-
447 crystallin: Differences in stability, subunit exchange and chaperone activity of homo and mixed
448 oligomers of αb-crystallin and its phosphorylation-mimicking mutant. J Mol Biol 375:1040-
449 1051.

450 Balch, WE, Morimoto, RI, Dillin, A and Kelly, JW (2008). Adapting proteostasis for disease
451 intervention. Science 319:916-919.

452 Benesch, JLP, Ayoub, M, Robinson, CV and Aquilina, JA (2008). Small heat shock protein activity is
453 regulated by variable oligomeric substructure. J Biol Chem 283:28513-28517.

454 Bertoncini, CW, Jares-Erijman, EA, Jovin, TM, Klement, R and Roberti, MJ (2007). Fluorescence
455 imaging of amyloid formation in living cells by a functional, tetracysteine-tagged alpha-
456 synuclein. Nat Methods 4:345-351.

457 Bova, MP, Ding, LL, Horwitz, J and Fung, BKK (1997). Subunit exchange of αa-crystallin. J Biol Chem
458 272:29511-29517.

459 Bova, MP, Mchaourab, HS, Han, Y and Fung, BKK (2000). Subunit exchange of small heat shock
460 proteins: Analysis of oligomer formation of alphaa-crystallin and hsp27 by fluorescence
461 resonance energy transfer and site-directed truncations. J Biol Chem 275:1035-1042.

462 Brown, JWP, Buell, AK, Michaels, TCT, Meisl, G, Carozza, J, Flagmeier, P, Vendruscolo, M, Knowles,
463 TPJ, Dobson, CM and Galvagnion, C (2016). B-synuclein suppresses both the initiation and
464 amplification steps of α-synuclein aggregation via competitive binding to surfaces. Scientific
465 reports 6:36010.

466 Bruinsma, IB, Bruggink, KA, Kinast, K, Versleijen, AAM, Segers-Nolten, IMJ, Subramaniam, V, Bea
467 Kuiperij, H, Boelens, W, de Waal, RMW and Verbeek, MM (2011). Inhibition of alpha-synuclein
468 aggregation by small heat shock proteins. Proteins Struct Funct Bioinformat 79:2956-2967.

469 Carra, S, Rusmini, P, Crippa, V, Giorgetti, E, Boncoraglio, A, Cristofani, R, Naujock, M, Meister, M,
470 Minoia, M, Kampinga, HH and Poletti, A (2013). Different anti-aggregation and pro-
471 degradative functions of the members of the mammalian shsp family in neurological
472 disorders. Philos Trans R Soc Lond B Biol Sci 368.

473 Chai, YJ, Sierecki, E, Tomatis, VM, Gormal, RS, Giles, N, Morrow, IC, Xia, D, Götz, J, Parton, RG,
474 Collins, BM, Gambin, Y and Meunier, FA (2016). Munc18-1 is a molecular chaperone for α-
475 synuclein, controlling its self-replicating aggregation. The Journal of Cell Biology 214:705-718.

476 Chang, E and Kuret, J (2008). Detection and quantification of tau aggregation using a membrane
477 filter assay. Anal Biochem 373:330-336.

478 Cox, D, Carver, JA and Ecroyd, H (2014). Preventing α-synuclein aggregation: The role of the small
479 heat-shock molecular chaperone proteins. Biochim Biophys Acta (BBA) - Molecular Basis of
480 Disease 1842:1830-1843.

481 Cox, D, Selig, E, Griffin, MD, Carver, JA and Ecroyd, H (2016). Small heat shock proteins prevent
482 alpha-synuclein aggregation via transient interactions and their efficacy is affected by the rate
483 of aggregation. J Biol Chem.

484 Crivat, G and Taraska, JW (2012). Imaging proteins inside cells with fluorescent tags. Trends
485 Biotechnol 30:8-16.

486 Datskevich, PN and Gusev, NB (2014). Structure and properties of chimeric small heat shock proteins
487 containing yellow fluorescent protein attached to their c-terminal ends. Cell Stress
488 Chaperones 19:507-518.

Datskevich, PN, Mymrikov, EV and Gusev, NB (2012a). Utilization of fluorescent chimeras for investigation of heterooligomeric complexes formed by human small heat shock proteins. Biochimie 94:1794-1804.

Datskevich, PN, Mymrikov, EV, Sluchanko, NN, Shemetov, AA, Sudnitsyna, MV and Gusev, NB (2012b). Expression, purification and some properties of fluorescent chimeras of human small heat shock proteins. Protein Expr Purif 82:45-54.

de Jong, WW, Leunissen, JA and Voorter, CE (1993). Evolution of the alpha-crystallin/small heat-shock protein family. Mol Biol Evol 10:103-126.

de Lau, LML and Breteler, MMB (2006). Epidemiology of parkinson's disease. Lancet Neurol 5:525-535.

Dorsey, ER, Constantinescu, R, Thompson, JP, Biglan, KM, Holloway, RG, Kieburtz, K, Marshall, FJ, Ravina, BM, Schifitto, G, Siderowf, A and Tanner, CM (2007). Projected number of people with parkinson disease in the most populous nations, 2005 through 2030. Neurology 68:384-386.

Fioriti, L, Dossena, S, Stewart, LR, Stewart, RS, Harris, DA, Forloni, G and Chiesa, R (2005). Cytosolic prion protein (prp) is not toxic in n2a cells and primary neurons expressing pathogenic prp mutations. J Biol Chem 280:11320-11328.

Földi, I, Tóth, AM, Szabó, Z, Mózes, E, Berkecz, R, Datki, ZL, Penke, B and Janáky, T (2013). Proteome-wide study of endoplasmic reticulum stress induced by thapsigargin in n2a neuroblastoma cells. Neurochem Int 62:58-69.

Gui, M-c, Chen, B, Yu, S-s and Bu, B-t (2014). Effects of suppressed autophagy on mitochondrial dynamics and cell cycle of n2a cells. Journal of Huazhong University of Science and Technology [Medical Sciences] 34:157-160.

Guo, F, He, X-B, Li, S and Le, W (2016). A central role for phosphorylated p38α in linking proteasome inhibition-induced apoptosis and autophagy. Mol Neurobiol:1-13.

Hoyer, W, Cherny, D, Subramaniam, V and Jovin, TM (2004). Impact of the acidic c-terminal region comprising amino acids 109−140 on α-synuclein aggregation in vitro. Biochemistry 43:16233-16242.

Jehle, S, Rajagopal, P, Bardiaux, B, Markovic, S, Kuhne, R, Stout, JR, Higman, VA, Klevit, RE, van Rossum, BJ and Oschkinat, H (2010). Solid-state nmr and saxs studies provide a structural basis for the activation of alphab-crystallin oligomers. Nat Struct Mol Biol 17:1037-1042.

Jehle, S, Vollmar, BS, Bardiaux, B, Dove, KK, Rajagopal, P, Gonen, T, Oschkinat, H and Klevit, RE (2011). N-terminal domain of αb-crystallin provides a conformational switch for multimerization and structural heterogeneity. Proc Natl Acad Sci U S A.

Juenemann, K, Wiemhoefer, A and Reits, EA (2015). Detection of ubiquitinated huntingtin species in intracellular aggregates. Front Mol Neurosci 8:1.

Kampinga, H, Hageman, J, Vos, M, Kubota, H, Tanguay, R, Bruford, E, Cheetham, M, Chen, B and Hightower, L (2009). Guidelines for the nomenclature of the human heat shock proteins. Cell Stress Chaperon 14:105-111.

Kanda, S, Bishop, JF, Eglitis, MA, Yang, Y and Mouradian, MM (2000). Enhanced vulnerability to oxidative stress by α-synuclein mutations and c-terminal truncation. Neurosci 97:279-284.

Klucken, J, Shin, Y, Masliah, E, Hyman, BT and McLean, PJ (2004). Hsp70 reduces α-synuclein aggregation and toxicity. J Biol Chem 279:25497-25502.

Krishnan, J, Lemmens, R, Robberecht, W and Van Den Bosch, L (2006). Role of heat shock response and hsp27 in mutant sod1-dependent cell death. Exp Neurol 200:301-310.

533 Lelj-Garolla, B and Mauk, AG (2006). Self-association and chaperone activity of hsp27 are thermally
534 activated. J Biol Chem 281:8169-8174.

535 Li, W, West, N, Colla, E, Pletnikova, O, Troncoso, JC, Marsh, L, Dawson, TM, Jäkälä, P, Hartmann, T,
536 Price, DL and Lee, MK (2005). Aggregation promoting c-terminal truncation of α-synuclein is a
537 normal cellular process and is enhanced by the familial parkinson's disease-linked mutations.
538 Proc Natl Acad Sci U S A 102:2162-2167.

539 Massano, J and Bhatia, KP (2012). Clinical approach to parkinson's disease: Features, diagnosis, and
540 principles of management. Cold Spring Harb Perspect Med 2:a008870.

541 Matsuzaki, M, Hasegawa, T, Takeda, A, Kikuchi, A, Furukawa, K, Kato, Y and Itoyama, Y (2004).
542 Histochemical features of stress-induced aggregates in α-synuclein overexpressing cells. Brain
543 Res 1004:83-90.

544 McLean, PJ, Kawamata, H and Hyman, BT (2001). A-synuclein–enhanced green fluorescent protein
545 fusion proteins form proteasome sensitive inclusions in primary neurons. Neurosci 104:901-
546 912.

547 Nasir, I, Linse, S and Cabaleiro-Lago, C (2015). Fluorescent filter-trap assay for amyloid fibril
548 formation kinetics in complex solutions. ACS Chemical Neuroscience 6:1436-1444.

549 Ojha, J, Masilamoni, G, Dunlap, D, Udoff, RA and Cashikar, AG (2011). Sequestration of toxic
550 oligomers by hspb1 as a cytoprotective mechanism. Mol Cell Biol 31:3146-3157.

551 Olshina, MA, Angley, LM, Ramdzan, YM, Tang, J, Bailey, MF, Hill, AF and Hatters, DM (2010). Tracking
552 mutant huntingtin aggregation kinetics in cells reveals three major populations that include an
553 invariant oligomer pool. J Biol Chem 285:21807-21816.

554 Ormsby, AR, Ramdzan, YM, Mok, Y-F, Jovanoski, KD and Hatters, DM (2013). A platform to view
555 huntingtin exon 1 aggregation flux in the cell reveals divergent influences from chaperones
556 hsp40 and hsp70. J Biol Chem 288:37192-37203.

557 Ostrerova-Golts, N, Petrucelli, L, Hardy, J, Lee, JM, Farer, M and Wolozin, B (2000). The a53t α-
558 synuclein mutation increases iron-dependent aggregation and toxicity. J Neurosci 20:6048-
559 6054.

560 Outeiro, TF, Klucken, J, Strathearn, KE, Liu, F, Nguyen, P, Rochet, J-C, Hyman, BT and McLean, PJ
561 (2006). Small heat shock proteins protect against α-synuclein-induced toxicity and
562 aggregation. Biochem Biophys Res Commun 351:631-638.

563 Paxinou, E, Chen, Q, Weisse, M, Giasson, BI, Norris, EH, Rueter, SM, Trojanowski, JQ, Lee, VM and
564 Ischiropoulos, H (2001). Induction of alpha-synuclein aggregation by intracellular nitrative
565 insult. J Neurosci 21:8053-8061.

566 Ramdzan, YM, Polling, S, Chia, CPZ, Ng, IHW, Ormsby, AR, Croft, NP, Purcell, AW, Bogoyevitch, MA,
567 Ng, DCH, Gleeson, PA and Hatters, DM (2012). Tracking protein aggregation and
568 mislocalization in cells with flow cytometry. Nat Methods 9:467-470.

569 Van Montfort, R, Slingsby, C and Vierling, E (2002). Structure and function of the small heat shock
570 protein/alpha-crystallin family of molecular chaperones. Adv Protein Chem 59:105-156.

571 Wan, OW and Chung, KKK (2012). The role of alpha-synuclein oligomerization and aggregation in
572 cellular and animal models of parkinson's disease. PLoS ONE 7:e38545.

573 Yerbury, JJ, Stewart, EM, Wyatt, AR and Wilson, MR (2005). Quality control of protein folding in
574 extracellular space. EMBO Rep 6:1131-1136.

575 Zourlidou, A, Payne Smith, MD and Latchman, DS (2004). Hsp27 but not hsp70 has a potent
576 protective effect against α-synuclein-induced cell death in mammalian neuronal cells. J
577 Neurochem 88:1439-1448.

578

Figure Legends

Figure 1: Expression of fluorescently tagged α-syn isoforms does not result in a substantial number of N2a or HEK293 cells with inclusions. N2a or HEK293 cells were transiently transfected with constructs encoding for EGFP (negative control), TDP-43-tGFP (positive control) or EGFP-tagged variants of α-synWT or α-synA53T. Cells were treated with proteostasis inhibitors (10 μM MG132, 3 μM thapsigargin, or 10 mM FeCl2) as indicated and incubated for 48 h before being mounted on glass slides and imaged via confocal microscopy. Images were randomly collected according to the brightfield channel, and the number of EGFP-positive cells containing diffuse or aggregated fluorescent protein was manually quantified using (A, right panel) an overlay of the brightfield and fluorescent images. Examples of cells counted as (1) diffuse fluorescence and (2) punctate fluorescence are shown. Scale bars represent 25 μm, and 5 μm in inset. The percentage of EGFP-positive cells containing inclusions for (B) N2a or (C) HEK293 cells following each treatment is displayed as mean ± S.E.M. (n=3), and was analysed via a one-way ANOVA with a Dunnett's post-test compared to the untreated EGFP control, where *** indicates $p<0.001$.

Figure 2: α-synA53T* forms punctate inclusions in N2a cells. N2a cells were transiently transfected with a construct expressing α-synA53T* and incubated for 48 hours before being treated (or not) with 3-MA (10 mM), MG132 (10 μM) or an equivalent volume of the vehicle control (DMSO) and incubated for a further 48 hours. Intracellular α-syn was fluorescently labelled via immunohistochemistry, using a monoclonal mouse anti-αsyn antibody and a DyLight650-conjugated anti-mouse secondary antibody. (A-D) Fluorescent images of cells containing both cytosolic intracellular (A, B) and membrane-localised (C, D) inclusions are presented. Scale bars represent 5 μm. (E) The percentage of cells containing inclusions was quantified by manually counting at least 50 transfected cells and the number of α-syn positive cells containing fluorescent inclusions enumerated. Data are displayed as mean ± S.E.M. (n=4), and was analysed via one-way ANOVA with

a Dunnett's multiple comparison post-test, where * indicates $p<0.05$ compared to untreated or DMSO-treated controls. (F) Monomeric or fibrillar recombinant α-syn was added at various concentrations (0 – 0.5 μM) to either 50 mM phosphate buffer (pH 7.4) or 200 μg of untransfected cell lysate. Samples were analysed via filter trap using a 0.2 μm membrane, and detected using a monoclonal mouse anti-α-syn followed by a HRP-conjugated secondary antibody. (G) Cell extracts prepared from (i) mock transfected cells, and cells transfected with (ii) an EGFP vector control or (iii) the α-synA53T* construct. Cells were incubated in the absence (Untreated) or presence (Treated) of proteostasis inhibitors (10 μM MG132 and 3 μM thapsigargin). Samples were analysed via filter trap using a 0.2 μm membrane, and detected using a monoclonal mouse anti-α-syn followed by a HRP-conjugated secondary antibody. Samples in F and G were analysed on the one membrane, and the image from this membrane has been truncated for clarity.

Figure 3: sHsps are overexpressed following transfection with IRES bicistronic constructs. N2a cells were mock transfected (A, C), or transiently transfected with IRES constructs expressing (B) EGFP/αB-c or (D) EGFP/Hsp27. Forty-eight hours following transfection, cells were immunolabelled for intracellular sHsps using polyclonal rabbit anti-sHsp antibodies. Transfected cells were identified via EGFP fluorescence, and sHsps were visualised using DyLight650-conjugated secondary antibodies. Scale bars represent 25μm.

Figure 4: sHsps inhibit the formation of α-syn inclusions in cells. N2a cells were transiently transfected with a construct expressing α-synA53T*, along with an IRES construct expressing EGFP/αB-c, EGFP/Hsp27 or EGFP/EGFP^{inv}. Forty-eight hours following transfection, cells were treated with MG132 and thapsigargin (10 μM and 3 μM, respectively) or 3-MA (10 mM), then incubated for a further 48 h. Intracellular α-syn was immunohistochemically labelled, using a monoclonal mouse anti-αsyn antibody and a DyLight650-conjugated secondary antibody. (A) Cells containing αB-c

display EGFP fluorescence, and (B) α-syn positive cells display red fluorescence. (C) Fluorescence images overlayed on the brightfield channel allow automated detection and selection of co-transfected cells. (D) The percentage of co-transfected cells containing inclusions was quantified by manually selecting cells positive for α-syn expression and containing inclusions, and then removing cells that were not co-transfected. Data is displayed as mean ± S.E.M. (n=3 biological repeats, each consisting of at least 50 cells), and was analysed via two-way ANOVA with a Bonferroni post-test, where * indicates $p<0.05$ and ** indicates $p<0.01$ within treatment groups when compared to the $EGFP^{inv}$ control.

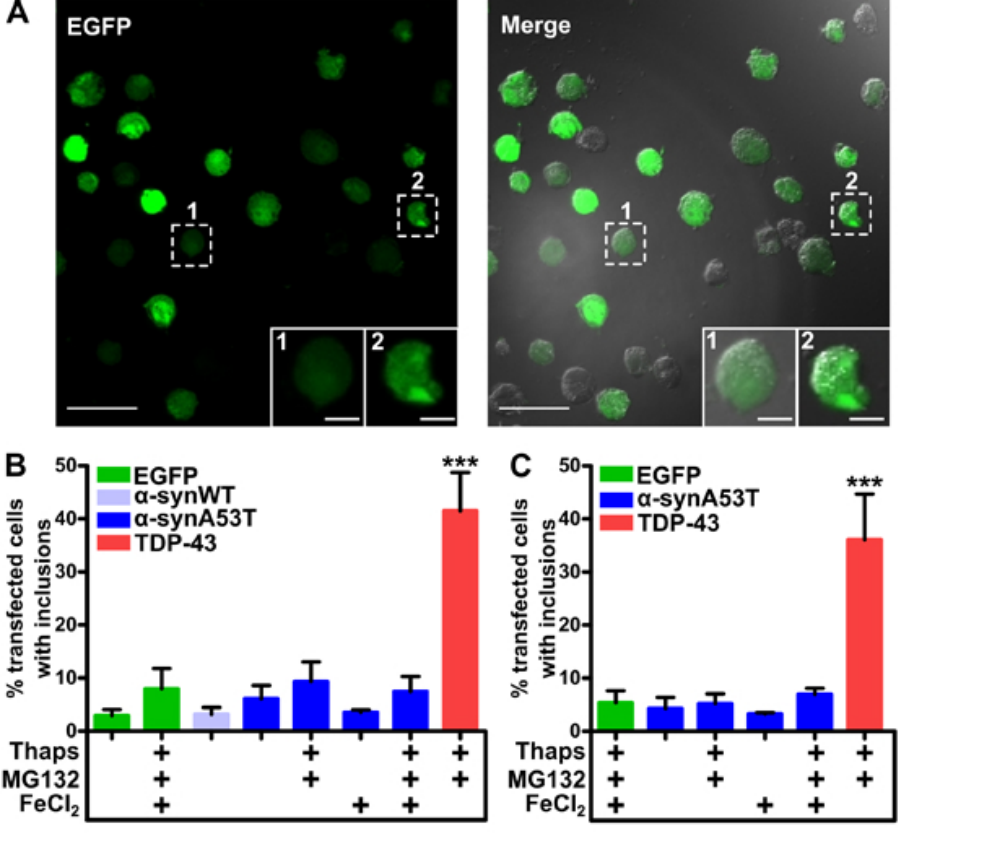
A
EGFP
Merge
1
2
B
EGFP
α-synWT
α-synA53T
TDP-43
% transfected cells with inclusions
***
Thaps
MG132
FeCl2
C
EGFP
α-synA53T
TDP-43
% transfected cells with inclusions
***
Thaps
MG132
FeCl2

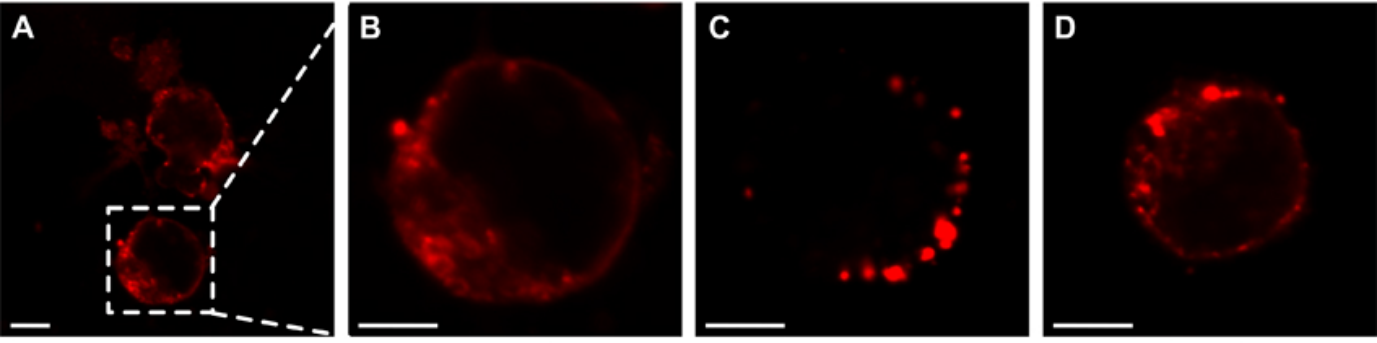
A
B
C
D

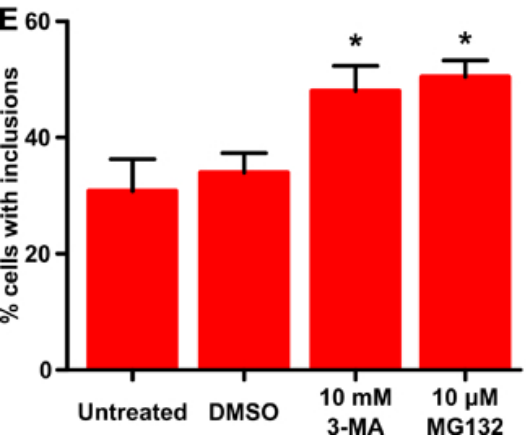
E
% cells with inclusions
60
40
20
0
*
*
Untreated
DMSO
10 mM 3-MA
10 μM MG132

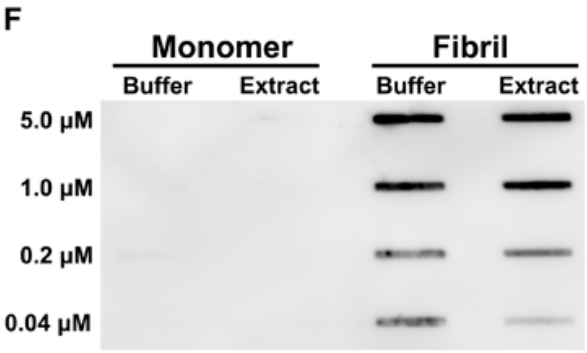
F
Monomer
Fibril
Buffer
Extract
Buffer
Extract
5.0 μM
1.0 μM
0.2 μM
0.04 μM

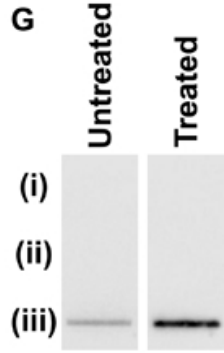
G
Untreated
Treated
(i)
(ii)
(iii)

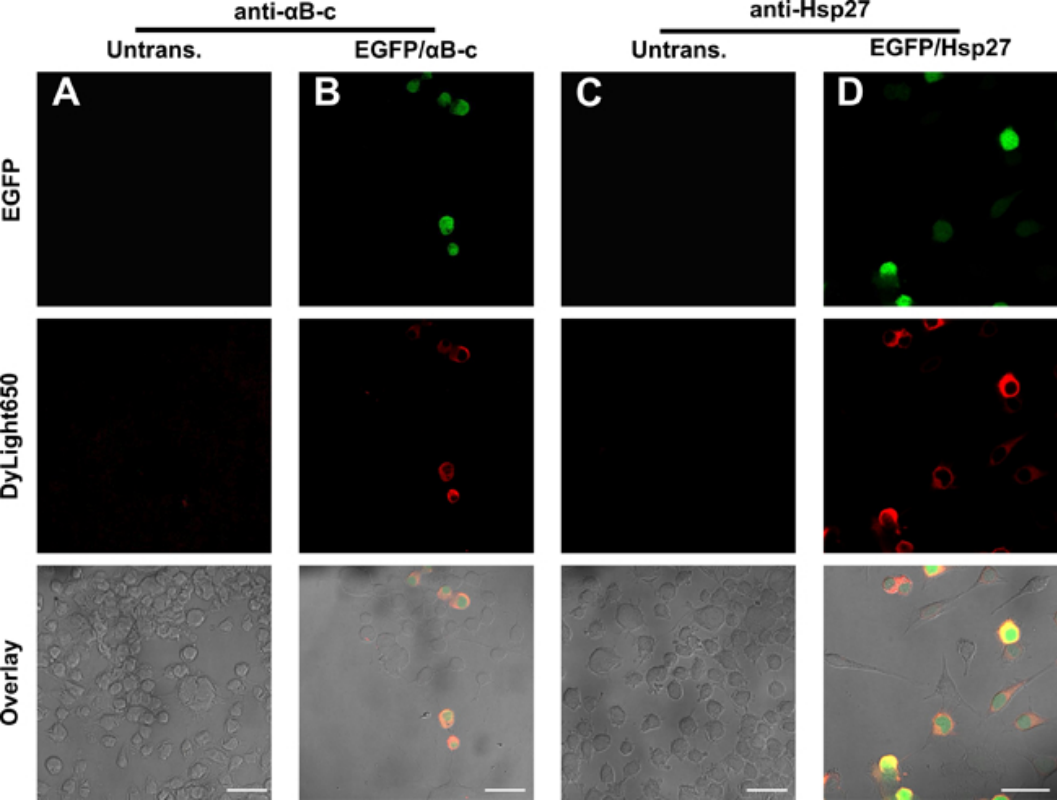
anti-αB-c
anti-Hsp27
Untrans.
EGFP/αB-c
Untrans.
EGFP/Hsp27
A
B
C
D
EGFP
DyLight650
Overlay

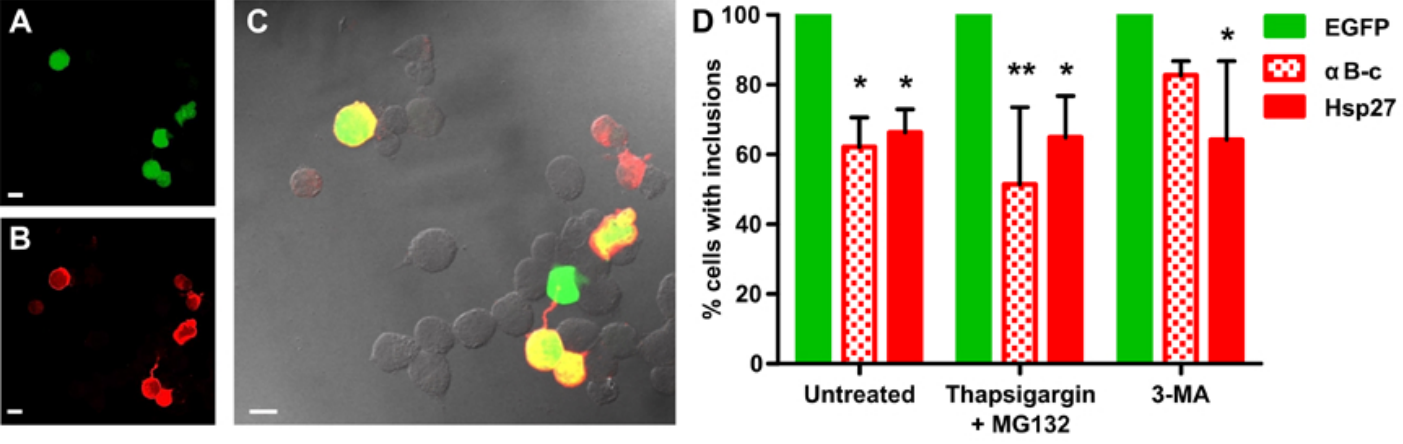
A
B
C
D
% cells with inclusions
100
80
60
40
20
0
*
*
**
*
*
EGFP
α B-c
Hsp27
Untreated
Thapsigargin
+ MG132
3-MA